Application Note
OCT 2022
AN-850-0128

Characterizing Amyloid-Forming Immunoglobulin G Light and Variable Chains Using Microfluidic Modulation Spectroscopy

- ○ Biosimilars
- ✓ mAbs
- ○ ADCs
- ○ AAVs
- ○ Ligand Binding
- ✓ Protein/Peptide Analysis
- ○ VLPs
- ○ Nucleic Acid
- ○ Fusion Proteins
- ○ Enzyme Analysis

- ✓ Aggregation
- Quantitiation
- ✓ Structure
- ✓ Stability
- Similarity

www.redshiftbio.com

Introduction

Immunoglobulin G (IgG) glycoproteins are produced in white blood cells and are among the most prevalent proteins in human serum.[1] IgGs are composed of two heavy chains and two lights chains (LCs) (Figure 1). LCs are approximately 215 amino acids in length and are organized into 2 domains: a variable (V_L) and a constant (C_L) domain, both primarily consisting of beta-sheets. In certain pathological conditions, some IgG LCs may be overexpressed and misfolded.[2]

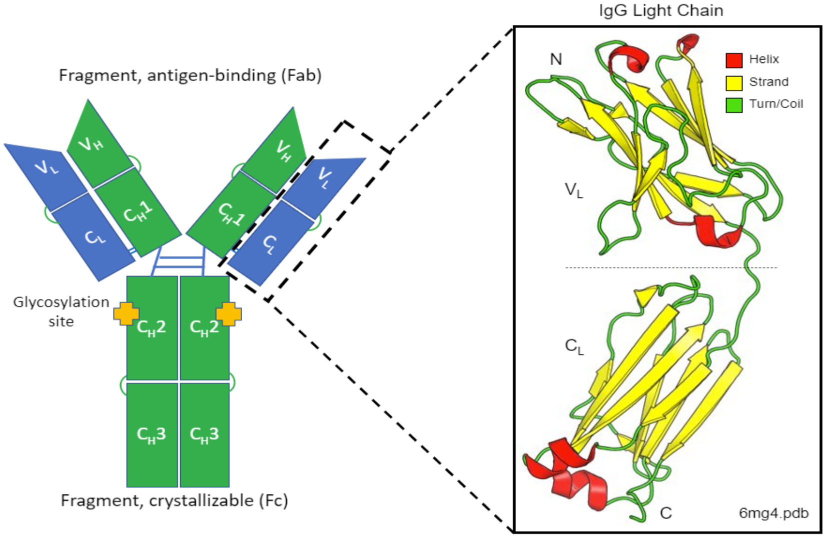

	HOS%	
	LC	V_L
Coil/Turn	44.2	49.5
Strand	47.4	44.9
Helix	8.4	5.6

Figure 1. A schematic representation of an IgG (left) and the X-ray crystal structure (center) of the light chain (PDB: 6mg4). [3] The higher-order structure (HOS) composition is shown in the table at the right.

Light Chain Amyloidosis is the life-threatening disease, which is the most common type of systemic amyloidosis, occurring when misfolded aggregates of LCs, called amyloids, deposit in extracellular locations.[4] Although all LCs share the same fold only some isoforms are prone to aggregation and lead to amyloidosis. The mechanism that converts soluble LCs to fibrillar aggregates has not been elucidated, although it is believed that aggregation is accelerated by destabilizing the native structure. Structural characterization of LCs found in patients with amyloidosis can help elucidate the aggregation mechanism and provide therapeutic insights.

In a recent study, researchers compared IgG light chains from non-disease-causing germline (GL) to potential disease-causing light chains from patients with multiple myeloma (MM) and from amyloidosis patients (AL).[4] Specific mutations in the variable domain from amyloidosis isoforms were found which make the LC more flexible and solvent-exposed and may therefore be a possible driver for fibril formation. The full-length LCs and the isolated variable domains from these three sources (GL, MM, and AL) were tested using Microfluidic Modulation Spectroscopy (MMS) to determine the secondary structural differences and the HOS composition. Since MMS can quantitate percent alpha-helix, beta-sheet, unordered (coil), and turn structures, the flexibility can also be inferred through increases in the unordered and turn structures.

MMS interrogates the Amide I band of the IR spectrum to sensitively probe protein structure while modulating against the reference buffer for accurate background subtraction in aqueous-based samples.[6] This technique is particularly sensitive to changes in beta-sheet structure over other techniques as it can distinguish between native beta-sheets (intramolecular) and aggregated beta-sheets (intermolecular), a distinction that is critical for monitoring the progression of amyloid formation.[7] The AQS³pro was used for this study and is equipped with a high-power Quantum Cascade Laser that is significantly brighter than traditional FTIR light sources. The combination of the brighter light source and modulating background subtraction makes MMS about 30 times more sensitive than FTIR and 5 times more sensitive than CD to small changes in structure.[8]

Methods

MMS: The full LC and its isolated variable domain were prepared from the three different cell lines investigated: germline (GL), multiple myeloma (MM), and amyloidosis (AL). Each sample was prepared at 0.5 mg/mL in 10 mM phosphate buffer, pH 7.5, containing 150 mM NaCl and run in duplicate on the AQS^{3}pro using a 5 psi backing pressure and 1 Hz modulation rate. All spectra were analyzed in duplicate and then averaged.

CD: Far-UV CD spectra and the melting data were recorded using a Jasco J-815 spectropolarimeter. CD spectra were recorded at 195-250 nm from samples containing 0.4 mg/mL protein placed in 1 mm quartz cells. Following the baseline subtraction, the spectra were smoothed using a noise-reduction routine. The data were normalized to protein concentration and expressed in units of molar residue ellipticity (MRE).

Results

Using MMS, the spectral changes at wavenumbers 1640 cm^{-1} (native beta-sheet) and 1656 cm^{-1} (alpha-helix) were tracked for the isolated variable domains (GL V$_L$, AL V$_L$, MM V$_L$) and full-length light chains (GL LC, AL LC, MM LC) and compared to the GL LC sample. The results for these samples are shown in Figure 2, and they are clearly distinguishable from each other due to the increase in fractional beta-sheet content and decrease in alpha-helical content in the variable chain. These results are consistent with the crystal structure shown in Figure 1 and HOS table which show the variable chain has very little alpha-helical content.

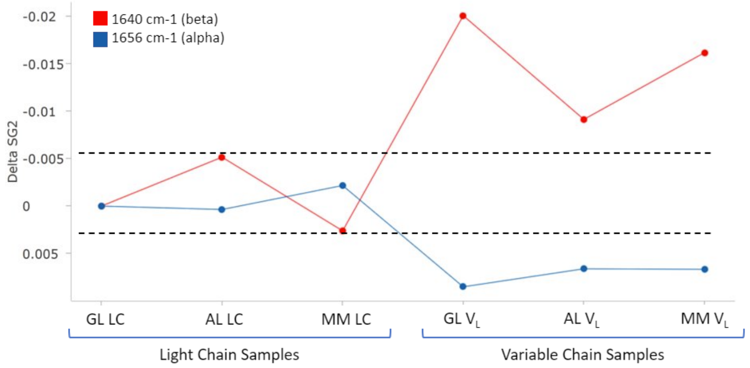

Figure 2. The isolated variable domains (V$_L$) from germline (GL), multiple myeloma (MM) and amyloidosis (AL) on the right were clearly distinguishable from each other and from intact light chain (LC) samples on the left. Changes were tracked by monitoring the signal at the 1640 cm^{-1} and 1656 cm^{-1} regions of the IR spectrum known for native beta-sheet and alpha-helix, respectively.

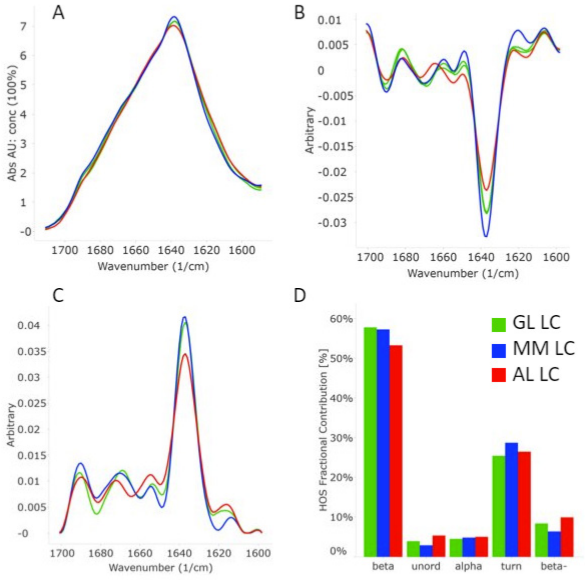

Figure 3. LC sample results including A) absolute absorbance, B) The second derivative, C) The similarity plot, and D) the HOS fractional contributions.

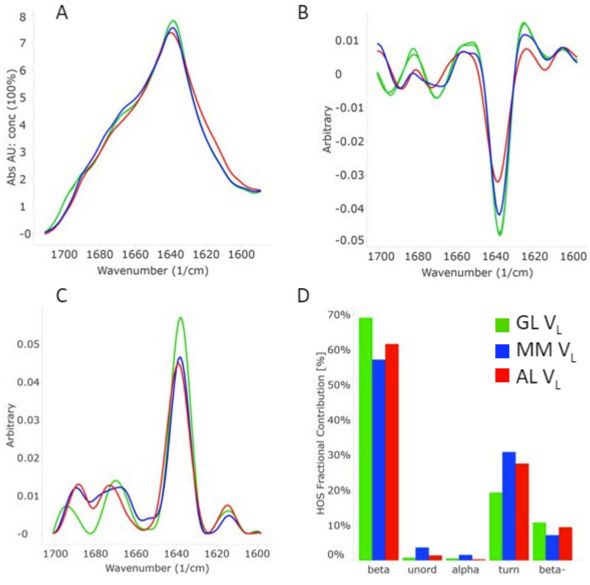

Figure 4. V$_L$ sample results including A) absolute absorbance, B) The second derivative, C) The similarity plot, and D) the HOS fractional contributions.

Application Note
OCT 2022

Results, continued

The HOS bar graphs were combined in Figure 5 to show the side-by-side comparison of the LC and V_L for GL, MM, and AL. The color pattern remains the same where GL is green, MM is blue, and AL is red. The shading now differentiates the LC and V_L samples where the LC samples are the brighter shades and the V_L samples are the darker shades.

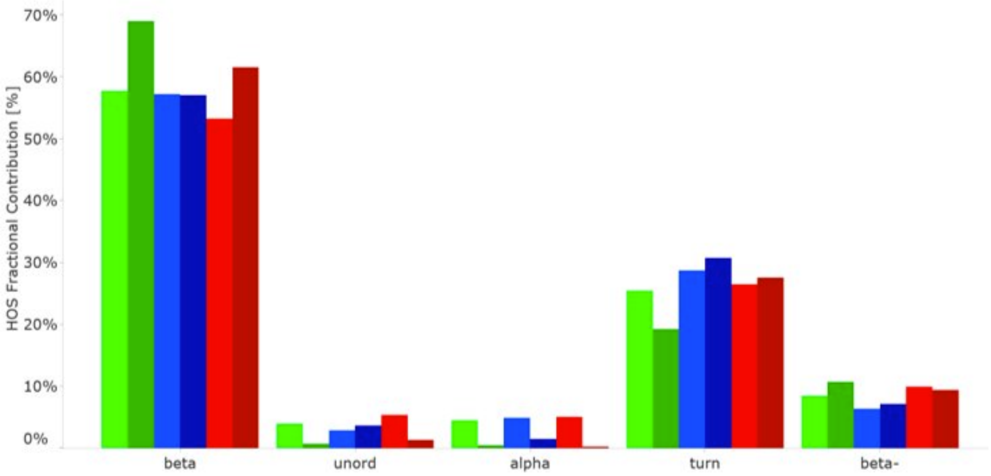

	Sample Name	% beta	% unord	% alpha	% turn	% beta-
🟩	GL LC	58	4	4	25	8
🟩	GL V_L	69	1	0	19	11
🟦	MM LC	57	3	5	29	6
🟦	MM V_L	57	4	1	31	7
🟥	AL LC	53	5	5	26	10
🟥	AL V_L	62	1	0	28	9

Figure 5. All samples HOS. GL samples are green, MM are blue, and AL are red. The LC samples are the lighter shades and the V_L samples are the darker shades.

Secondary structure contribution was also probed using circular dichroism (CD) and is shown in Figure 6 for the LC samples (A) and the V_L samples (B). All spectra showed a prevalence of beta-sheet secondary structure, where the minimum is at 215 nm, in agreement with the IgG fold. However, deconvoluting CD spectra is not as straightforward due to overlapping regions of alpha-helix and beta-sheet and the large disparity in signal, as seen in Figure 7. Therefore, fractional contribution of HOS was not calculated. The CD signal for alpha-helical structures is much more prominent than beta-sheet, additionally, inter and intramolecular beta-sheets cannot be distinguished with CD. These spectra were used as qualitative tools for making comparisons and monitoring trends only.

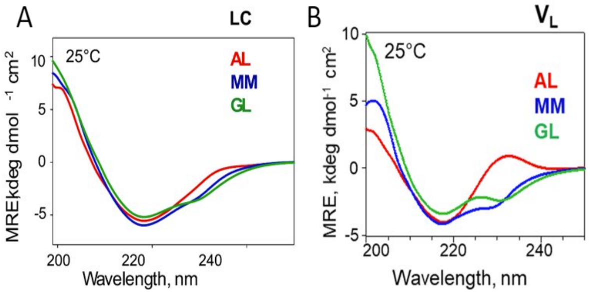

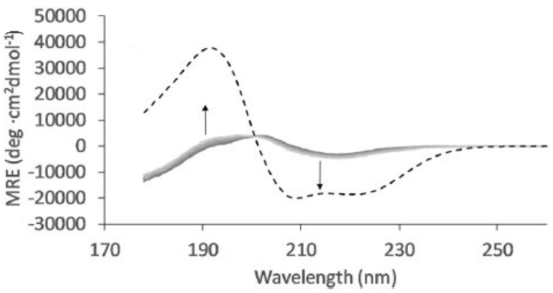

Figure 6. CD spectra of (A) LC and (B) V_L samples show similar trends between the AL, MM, and GL samples in the light and variable chains.

Figure 7. CD spectra of IgG (solid lines, beta-sheet structure) and BSA (dashed line, alpha-helix structure). Both were 1 mg/mL, however, the BSA sample has a much more intense signal.[7]

Application Note
OCT 2022

Conclusions

Structural characterization of amyloid-forming proteins is crucial to understanding the aggregation mechanisms in amyloidosis and developing effective therapeutic strategies. In this study, we compared LC and V_L fragments from three different amyloidogenic and non-amyloidogenic sources. Those three sources were GL (non-amyloidogenic), MM (possibly amyloidogenic), and AL (amyloidogenic). The HOS determined by MMS was similar to the results gathered from X-ray crystallography (Figure 1). Although the MMS data do not have the resolution of an X-ray crystal structure, the data collection and processing are significantly faster and easier, which provides a quantitative and immediate result of protein HOS. Moreover, being an in-solution technique, it is capable of detecting subtle structural differences that may not be visible in the crystalline state.

We found that the LC samples contained more alpha-helical content than the V_L samples, making them easy to distinguish from the V_L samples. The AL samples generally contained less beta-sheet structure and more unordered structure than the non-amyloidogenic forms, in agreement with the greater flexibility and solvent exposure shown in previous work. AL also showed more pronounced intermolecular beta-sheet structure than the other samples, aside from the GL V_L sample, which is a result of the signal around the 1697 cm^{-1} region that is unique to that sample. General qualitative trends were observed in the CD structural results, and due to the nature of the measurement and poor sensitivity for beta-sheet content, no quantitative conclusions could be made. In summary, MMS provided quantitative HOS characterization and the ability to distinguish between native and aggregation-prone beta-sheet structures, which are important for the study of amyloidogenic proteins.

Primary Author: Valerie Collins, Ph.D.

CONTRIBUTOR(S):

Northeastern University
360 Huntington Ave, Boston, MA 02115.

References

1. Vidarsson, Gestur, Gillian Dekkers, and Theo Rispens. "IgG subclasses and allotypes: from structure to effector functions." Frontiers in immunology 5 (2014): 520.
2. Merlini, Giampaolo, and Vittorio Bellotti. "Molecular mechanisms of amyloidosis." New England Journal of Medicine 349.6 (2003): 583-596.
3. Morgan, Gareth J., *et al.* "Stabilization of amyloidogenic immunoglobulin light chains by small molecules." Proceedings of the National Academy of Sciences 116.17 (2019): 8360-8369.
4. Merlini, Giampaolo, *et al.* "Systemic immunoglobulin light chain amyloidosis." Nature reviews Disease primers 4.1 (2018): 1-19
5. Peterle, Daniele, *et al.* "A Conservative Point Mutation in a Dynamic Antigen-binding Loop of Human Immunoglobulin λ6 Light Chain Promotes Pathologic Amyloid Formation." Journal of Molecular Biology 433.24 (2021): 167310.
6. Ivancic, Valerie A., *et al.* "Advancing secondary structure characterization of monoclonal antibodies using Microfluidic Modulation Spectroscopy." Analytical Biochemistry 646 (2022): 114629.
7. Ivancic, V. Detection of Pressure-Induced Aggregation Using Mucrofluidic Modulation Spectroscopy (Application Note: AN-850-0109). Redshift BioAnalytics 2021. https://doi.org/https://www.redshiftbio.com/resources/detection-of-pressure-induced-protein-aggregation-with-mms.
8. Kendrick, Brent S., *et al.* "Determining spectroscopic quantitation limits for misfolded structures." Journal of pharmaceutical sciences 109.1 (2020): 933-936.